Formation of the isomeric pair $^{194}Ir^{m,g}$ in interactions of α particles with ^{192}Os

M. S. Uddin,[1,*] S. Sudár,[1,2] and S. M. Qaim[1,†]

[1]*Institut für Neurowissenschaften und Medizin, INM-5: Nuklearchemie, Forschungszentrum Jülich, D-52425 Jülich, Germany*

[2]*Institute of Experimental Physics, Debrecen University, H-4001 Debrecen, Hungary*

(Received 18 August 2010; revised manuscript received 3 March 2011; published 8 August 2011)

Cross sections were measured by the activation technique for the nuclear processes $^{192}Os(\alpha,d+pn+np)^{194}Ir^{m,g}$ up to α-particle energies of 39 MeV. From the measured data the isomeric cross-section ratio was deduced as a function of projectile energy. The present experimental data as well as those for the $^{194}Pt(n,p)^{194}Ir^{m,g}$ reaction, given in the literature, were compared with the results of nuclear model calculations using the code TALYS, which combines the statistical, precompound, and direct interactions. In general, the experimental data were reproduced well by the model calculations, which were done using relatively low values of η (i.e., $\Theta_{\rm eff}/\Theta_{\rm rigid}$). The results provide more evidence for the mass dependence of η. The level density parameter for ^{194}Ir was determined unambiguously.

DOI: 10.1103/PhysRevC.84.024605 PACS number(s): 24.60.Dr, 24.10.−i, 25.40.−h, 25.55.−e

I. INTRODUCTION

Studies of isomeric cross sections are of fundamental interest. It is known that the isomeric cross-section ratio, especially near the threshold of the reaction, is dependent on the spins of the levels involved, rather than on their separation energies [1,2]. Through detailed investigations on several isomeric pairs, involving different combinations of target, projectile, and ejectile, the effects of changes in the ratio of the effective moment of inertia to the rigid-body moment of inertia ($\eta = \Theta_{\rm eff}/\Theta_{\rm rigid}$), assumptions regarding the spin distribution after preequilibrium (PE) decay, and the role of input nuclear structure information have been elaborated [1–5].

The level density parameter **a**, a fundamental parameter for the model calculations, is determined from the measured mean *s*-wave neutron level spacing. The low-energy neutrons can excite only the levels of the compound nucleus having the spin of $I = I_t \pm 1/2$, where I_t is the spin of the ground state of the target nucleus. Therefore the level density parameter cannot be determined without knowing the spin distribution, i.e., the spin cutoff parameter and finally the previously defined η value. Since the introduction of the back-shifted Fermi gas model [6], the level density parameters are calculated for $\eta = 1.0$ and $\eta = 0.5$, but there is no strong experimental evidence that any of these values are valid. Furthermore, as a result of recent studies on the high-spin isomers $^{139}Nd^m$, $^{141}Nd^m$, $^{195}Hg^m$, and $^{197}Hg^m$ [7–9] it has been suggested that the η value is mass dependent (i.e., $\eta \neq$ const as it was supposed earlier). This suggestion is based on the low η value for mercury isotopes and somewhat higher value for the Nd isotopes, both being lower than 0.5. Other evidence is in [10], where for ^{51}V the value $\eta = 0.75$ was found and in [11] where a mass number dependence in the spin cutoff factor was shown from the analysis of the discrete levels (see the connection of their data to η in [8]). Now we report on the formation of the isomeric pair $^{194}Ir^{m,g}$ in α-particle-induced reactions on highly enriched ^{192}Os. The ground state $^{194}Ir^g$ ($T_{1/2} = 19.28 \pm 0.13$ h) has a low spin (1^-) and the metastable state $^{194}Ir^m$ ($T_{1/2} = 171.0 \pm 11$ d), lying at an excitation energy of <440 keV, has a higher spin (10,11). Both of them decay independently to ^{194}Pt, emitting β^- particles and several γ rays. The isomeric cross-section ratio has been previously measured for the $^{193}Ir(n,\gamma)^{194}Ir^{m,g}$ process [12] as well as for the $^{194}Pt(n,p)^{194}Ir^{m,g}$ reaction [13]. In both cases the value was <0.05. The present investigation had therefore two motivations: (a) to study the effect of higher angular momentum brought by the α particle on the isomer ratio, and (b) to provide more evidence for the mass dependence of η.

II. EXPERIMENT AND RESULTS

Cross sections of the $^{192}Os(\alpha,d+pn+np)^{194}Ir^{m,g}$ processes were measured as a function of the α-particle energy via the activation technique using the well-known stacked-foil irradiation arrangement. This involved irradiation of ^{192}Os targets and identification of the product radionuclides. The enriched ^{192}Os (99.65%; supplied by Chemotrade) targets were prepared by electrolytic deposition on 10-μm thick Ni backings. Several such targets and thin Ti (12.5 μm) foils, used as monitors as well as energy degraders, were irradiated together in a stack with a primary α-particle energy of 40 MeV at a beam current of 100 nA for 1 h at the CGR-560 cyclotron of the Vrije Universiteit Brussel (VUB), Brussels, Belgium. Due to the thin Ti foil in front of the stack, the effective α-particle energy in the first sample was 38.9 MeV. The beam flux was measured via the $^{nat}Ti(\alpha, x)^{51}Cr$ monitor reaction [14]. The details on target preparation, irradiation, beam flux monitoring, and chemical separation have already been reported in connection with the characterization of the therapeutic radionuclide $^{193}Pt^m$ via x-ray spectrometry [15]. The beam energy degradation along the stack was calculated using the computer program STACK, based on the

*Permanent address: Institute of Nuclear Science and Technology, Atomic Energy Research Establishment, GPO Box 3787, Dhaka-1000, Bangladesh.

†Corresponding author: s.m.qaim@fz-juelich.de

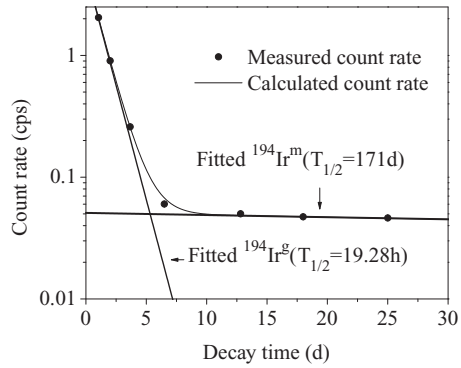

FIG. 1. Decrease in the count rate of the 328.45-keV γ ray as a function of decay time. The data were fitted with the known half-lives of the two independently decaying isomeric states $^{194}Ir^{m,g}$.

energy-range relationship. The Ir activity was measured by a HPGe detector with a digital γ-ray spectrometry system (ORTEC DSPEC jr ™) and GAMMAVISION data acquisition software. The sample-to-detector distance was 10 cm, whereby the effect of sample size on the efficiency and also the random coincidence loss became almost negligible. The radionuclide $^{194}Ir^{g}$ ($T_{1/2}$ = 19.28 h) was detected by the γ ray at energy 328.45 keV ($I_g = 13.1 \pm 0.4\%$). The metastable state $^{194}Ir^{m}$ ($T_{1/2} = 171.0\,d$) also produces the same γ ray ($I_m = 93 \pm 5\%$). The contributions of the two states were obtained by a decay curve analysis of the area under this γ-ray peak. A typical decay curve is given in Fig. 1.

The activity of the longer lived $^{194}Ir^{m}$ was measured after the complete decay of $^{194}Ir^{g}$. The counts of the γ rays at the energies 328.45 keV (93%), 338.8 keV (55%), and 482.83 keV (97%) were used to calculate the cross section of the $^{194}Ir^{m}$ formation. The decay data were taken from [16]. A good consistency was found among the results of those energies.

The count rate at the end of the bombardment (EOB) was converted to decay rate by introducing the necessary corrections for the efficiency of the detector and the intensity of the γ ray. For the counting geometry used, the random and true coincidence losses were negligible (<1%). From the decay rate and incident beam intensity, the cross section was calculated using the usual activation formula (cf., for example, [17]). The estimated uncertainties involved were similar to those given in [15]. The total uncertainty in the cross section obtained from the quadratic sum of individual uncertainties was 15%–20%. The isomeric cross-section ratio was calculated as the ratio of σ_m and σ_g. The uncertainty in the isomeric cross-section ratio was smaller, while dividing the formula for σ_m by σ_g and eliminating the common parameters we obtain:

$$\frac{\sigma_m}{\sigma_g} = \frac{\frac{C_0^m}{I_m(1-e^{\lambda_m T_{\rm irr}})}}{\frac{C_0^g}{I_g(1-e^{\lambda_g T_{\rm irr}})}},$$

where $C_0^{m,g}$ refer to the calculated EOB count rates of the decaying metastable and ground states, respectively. The preceding formula was used to deduce the uncertainties of the isomeric cross-section ratios, and the obtained values were 12%–17%. These include 8.95% uncertainty common to all energies which originated from the uncertainties of the half-lives and emission rate of the 328.45-keV γ ray. The covariance matrix of isomeric cross-section ratio was also created. The sources of uncertainties are summarized in Table I. The results of measurements and their uncertainties are given in Table II.

TABLE I. Sources of uncertainties in the measured cross sections of *m* and *g* states.

Source of uncertainty	Uncertainty (%)
Number of target nuclei	2
Target uniformity	5
Counting statistics	5–13
Efficiency of detector	4–6
Chemical yield determination	3
Half-life	0.7, 6.43
γ-ray intensity	3.1, 5.4
Monitor cross section (particle flux determination)	9–13
Total	15–20

III. NUCLEAR MODEL CALCULATIONS

Besides experimental studies, reaction cross sections were also calculated using the nuclear model code TALYS (version 1.2), which has been recently developed by Koning *et al*. [18]. It incorporates a number of nuclear models to analyze all the significant nuclear reaction mechanisms over the energy range of 1 keV–200 MeV. In the calculations, the particle transmission coefficients were generated via the spherical optical model using the ECIS-06 code [19] with global parameters for neutrons and protons from Koning and Delaroche [20]. For the optical model parameters (OMP) of complex particles (d, t, α, ^{3}He) the code made use of a folding approach, building up the OMPs from the neutron and proton potential. With these default OMPs for the incident α particle, the model underestimated the measured cross section as found previously [15]; therefore the OMPs were adjusted within

TABLE II. Activation cross sections of α-particle-induced reactions on ^{192}Os.

E_α (MeV)	$^{192}Os(\alpha,d)\ ^{194}Ir^{m,g}$[a]		
	$^{194}Ir^{m}$ (mb)	$^{194}Ir^{g}$ (mb)	σ_m/σ_g
38.9 ± 0.2	7.4 ± 1.0	21.0 ± 2.6	0.352 ± 0.029
37.9 ± 0.2	6.9 ± 1.0	20.0 ± 2.8	0.345 ± 0.030
37.5 ± 0.2	6.1 ± 1.0	19.9 ± 2.8	0.306 ± 0.029
36.4 ± 0.2	5.5 ± 0.9	19.1 ± 2.7	0.288 ± 0.028
35.1 ± 0.3	4.5 ± 0.7	16.1 ± 2.3	0.279 ± 0.030
34.5 ± 0.3	3.6 ± 0.6	13.4 ± 2.0	0.268 ± 0.031
32.6 ± 0.3	1.9 ± 0.4	8.8 ± 1.7	0.216 ± 0.035
32.5 ± 0.3	2.2 ± 0.4	8.7 ± 1.3	0.253 ± 0.031
31.8 ± 0.3	1.8 ± 0.3	8.3 ± 1.6	0.216 ± 0.028
30.6 ± 0.3	1.2 ± 0.2	5.7 ± 1.2	0.210 ± 0.029
29.9 ± 0.4	1.0 ± 0.2	5.2 ± 1.0	0.192 ± 0.027
27.8 ± 0.4	0.6 ± 0.1		

[a]Includes $^{192}Os(\alpha,pn+np)^{194}Ir^{m,g}$ reaction contributions.

their recommended limits to describe well the measured data. The γ-ray transmission coefficients were calculated through the energy-dependent γ-ray strength function according to Kopecky and Uhl [21] for E1 radiation, and according to Brink [22] and Axel [23] for all the other transition types. For the preequilibrium reactions a one-component exciton model of the TALYS code was used. The energies, spins, parities, and branching ratios of the discrete levels were based on the RIPL-2 database [24], which unfortunately does not contain the isomeric state $^{194}Ir^{m}$. It is missing, possibly because the energy of the level is not properly known. According to the Evaluated Nuclear Structure Data File (ENSDF), the energy of the level is $(190 + X)$ keV. We set $X = 0$. The experimental data were described well with this choice. In the continuum region the level density was calculated by the back-shifted Fermi gas model (BSFG) [6]. The **a** and Δ parameters of the BSFG for Pt isotopes were modified to get the best description of the measured cross section for the $^{192}Os(\alpha,n)^{195}Pt^{m}$ and $^{192}Os(\alpha,3n)^{193}Pt^{m}$ reactions [15]. In the present calculations those modified parameters were kept. In one output file of the TALYS code, the program sums up all the cross sections, calculated for various contributing routes, which lead to the same activation product isotope. Therefore the calculated result is comparable directly with the experimental value. The spin distribution of the level density was characterized by the ratio of the effective moment of inertia to the rigid-body moment of inertia ($\eta = \Theta_{\rm eff}/\Theta_{\rm rigid}$) and calculations were carried out for η values in the range of 0.15–1.0 in order to obtain the best fit to the experimentally determined isomeric-to-ground-state production ratio over the whole investigated energy range. Using the best η value, the level density parameter for the ^{194}Ir was determined and all calculations were repeated with the new level density parameter to get the final value for the η.

IV. DISCUSSION

A. Excitation functions and isomeric cross-section ratios

The experimental data for the $^{192}Os(\alpha,d+pn+np)^{194}Ir^{m,g}$ processes determined in this work are plotted as a function of the α-particle energy in Figs. 2–4. The results of nuclear model calculation using $\eta = 0.275$ are also shown in the same figures. In general, good agreement is found between the experimental and theoretically calculated excitation functions of the two isomeric states (Figs. 2 and 3), both in terms of shape and magnitude. The experimental isomeric cross-section ratio (σ_m/σ_g) is also reproduced very well by the model calculation (Fig. 4).

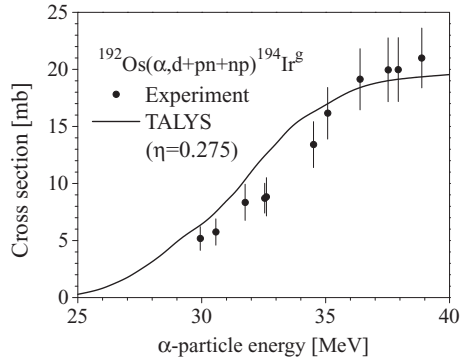

FIG. 2. Measured and calculated excitation function of the $^{192}Os(\alpha,d+pn+np)^{194}Ir^{g}$ process.

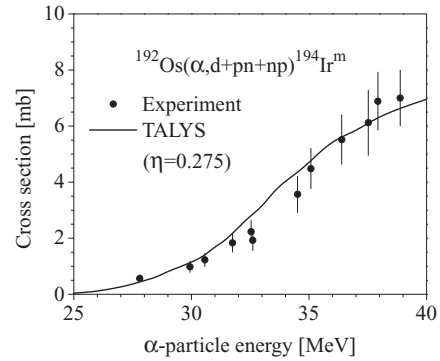

FIG. 3. Measured and calculated excitation function of the $^{192}Os(\alpha,d+pn+np)^{194}Ir^{m}$ process.

After completion of the investigation on the formation of the isomeric pair $^{194}Ir^{m,g}$ in the α-particle-induced process, we studied the formation of the same isomeric pair via another reaction available in the literature. The experimental data for the $^{194}Pt(n,p)^{194}Ir^{m,g}$ reaction reported in the literature are shown as a function of the neutron energy in Figs. 5–7. It should be noted that several groups [25–28] reported experimental cross sections for the $^{194}Ir^{g}$ with neutron energy around 14 MeV; but in only one laboratory [13] data for both the isomeric states were measured over a somewhat broader neutron energy range of 13.5–14.8 MeV. The results of nuclear model calculations done in this work are also given in Figs. 5–7. It should be noted that the neutron-induced reaction cross sections are much smaller than those for the α-particle-induced reactions.

For the $^{194}Pt(n,p)^{194}Ir^{g}$ reaction (Fig. 5) the experimental and theoretically calculated data agree very well. The results of the two data libraries (TENDL-2009 and ROSFOND-2010) are also shown. Apparently the ROSFOND-2010 curve shows better agreement with the experimental data, though the

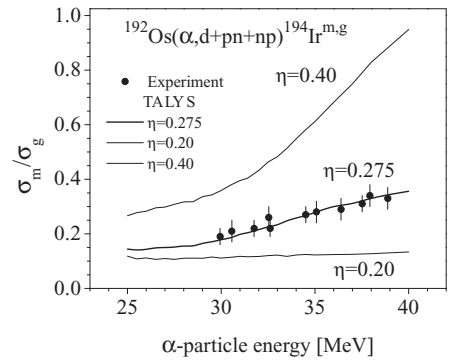

FIG. 4. Measured and calculated isomeric cross-section ratios of the $^{192}Os(\alpha,d+pn+np)^{194}Ir^{m,g}$ processes with the best $\eta = 0.275$ value, as well as with $\eta = 0.20$ and $\eta = 0.40$.

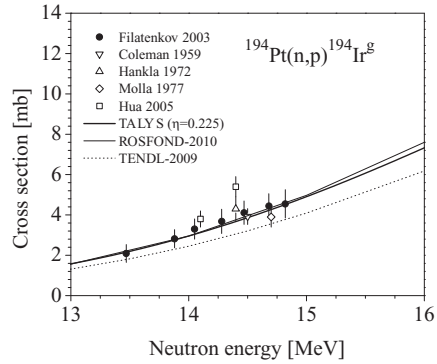

FIG. 5. Measured and calculated excitation function of the ^{194}Pt(n,p)^{194}Ir^{g} reaction. The measured data were taken from the literature (Filatenkov and Chuvaev [13], Coleman *et al.* [25], Hankla *et al.* [26], Molla and Qaim [27], Hua *et al.* [28]), and the result of nuclear model calculation (TALYS) is from this work.

TENDL-2009 curve also agrees within the lower limits of uncertainties of the experimental data, but it is systematically lower than the experimental data. As far as the ^{194}Pt(n,p)^{194}Ir^{m} reaction (Fig. 6) and the isomeric cross-section ratio (σ_m/σ_g) (Fig. 7) are concerned, the agreement between experiment and theory is fairly good. It should, however, be pointed out that in our calculation, also for this reaction a low value of η, i.e., 0.225, was necessary to reproduce the experimental data.

The isomeric cross-section ratios shown in Figs. 4 and 7 increase nearly linearly with the increasing projectile energy, thereby confirming the higher probability of formation of the higher spin isomer with the increasing excitation energy of the composite nucleus [1,2]. Furthermore, a comparison of the absolute values of the ratios (Figs. 4 and 7) depicts that the higher spin isomer is formed at least ten times more favorably in the α-particle-induced reaction than in the neutron-induced reaction. Thus the higher angular momentum brought by the α particle has a significant effect on the isomeric cross-section ratio.

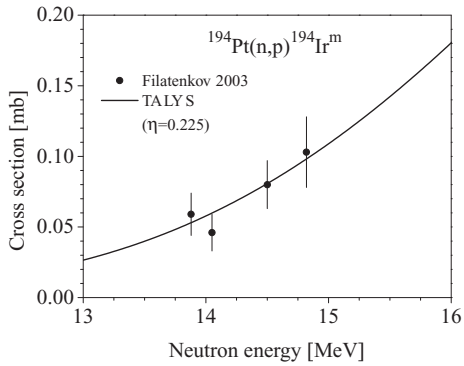

FIG. 6. Measured and calculated excitation function of the ^{194}Pt(n,p)^{194}Ir^{m} reaction. The measured data are from Filatenkov and Chuvaev [13] and the result of nuclear model calculation is from this work.

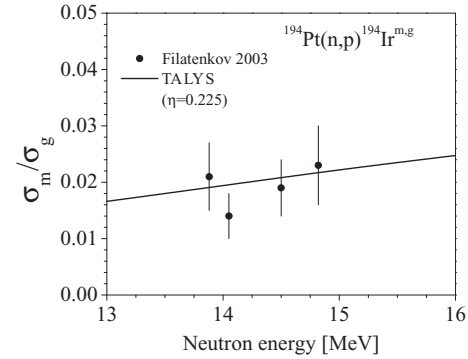

FIG. 7. Measured and calculated isomeric cross-section ratios of the ^{194}Pt(n,p)^{194}Ir^{m,g} reactions. The measured data are from Filatenkov and Chuvaev [13] and the result of nuclear model calculation is from this work.

B. Analysis of η values

The best η values were determined by analyzing the isomeric cross-section ratios as a function of the η value, by calculating the χ^2 value for N measurements which is defined for correlated data as

$$\chi^2(\eta) = [\vec{e} - \vec{c}(\eta)]^T M^{-1} [\vec{e} - \vec{c}(\eta)],$$

where $\vec{e} = [\ldots, \frac{\sigma_m(E_i)_{\rm exp}}{\sigma_g(E_i)_{\rm exp}}, \ldots]$, $\vec{c} = [\ldots, \frac{\sigma_m(E_i)_{\rm theor}}{\sigma_g(E_i)_{\rm theor}}, \ldots]$ are the vectors composed of the measured and calculated isomeric ratios; E_i is the incident energy, M^{-1} the inverse of the covariance matrix of the isomeric cross-section ratio, the indexes refer to experimental data or theoretical calculation, and T refers to the transposition of the vector. Figure 8 shows the "reduced" χ^2 values given by $\chi^2/(N-1)$.The best estimation for η is defined by the minimum value of the reduced χ^2. In the case of the ^{194}Pt(n,p)^{194}Ir^{m,g} reaction, the covariance information was not available, therefore it was approximated using the same 8.95% correlated uncertainties as in the case of our measurement. This underestimates the correlated uncertainties, as we were not able to remove some common error source. It can be seen in the figure that the ratio of the reduced χ^2 value of the maximum (at $\eta = 1.0$) to minimum of reduced χ^2 is 2610 for the α-particle-induced reaction and 9.96 for the neutron-induced reaction. This means

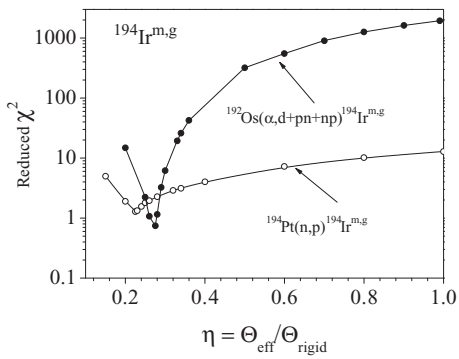

FIG. 8. The "reduced" χ^2value as a function of the η value used for the calculation of the isomeric cross-section ratio in the reactions ^{192}Os(α,$d+pn+np$)^{194}Ir^{m,g} and ^{194}Pt(n,p)^{194}Ir^{m,g}.

that the reduced χ^2 is 200 times more sensitive to the η value in the case of the α-particle-induced reaction. This is related to the higher angular momentum of the composite system in the former case. The η values for the minima of the reduced χ^2 values of both reactions are quite near to each other—exactly $\eta_{(\alpha,d)} = 0.275 \pm 0.02$ and $\eta_{(n,p)} = 0.225 \pm 0.04$. They are in agreement within the limits of uncertainties and the weighted average is $\eta = 0.265 \pm 0.018$, with the rounded value of 0.27 ± 0.02. This value is comparable, but significantly higher than that for the $^{195}Hg^m$ ($\eta = 0.15 \pm 0.05$) and $^{197}Hg^m$ ($\eta = 0.20 \pm 0.05$) nuclei [8] and gives more support to our postulate that η is mass dependent (that is, not constant), and it changes from nucleus to nucleus. For the general tendency very little data are available to make a plot, but from the data for ^{51}V ($\eta = 0.75$) [10] and our data a decreasing tendency with increasing mass number is presumable as deduced from the discrete levels [11].

We conclude that ^{194}Ir is the second nucleus for which, in the framework of the BSFG model, the level density parameters ($\mathbf{a}$,Δ) can be determined unambiguously. Using the experimental data, level spacing at 6.067 MeV and $\eta = 0.31 \pm 0.02$, and the discrete levels from the ENSDF library [29], we get $\mathbf{a} = (16.44 \pm 0.40)\frac{1}{\text{MeV}}$ and $\Delta = (-1.0 \pm 0.1)$ MeV.

To establish a usable mass dependence of η, further experimental investigation and model analysis is needed. The explanation of the mass dependence needs some deeper thoughts in the nuclear theory.

ACKNOWLEDGMENTS

We thank Prof. H.H. Coenen for his constant support and Prof. A. Hermanne for irradiations at the Brussels cyclotron. M.S. Uddin thanks the Alexander von Humboldt Foundation for financial support.

[1] S. M. Qaim, A. Mushtaq, and M. Uhl, Phys. Rev. C **38**, 645 (1988).
[2] F. Cserpák, S. Sudár, J. Csikai, and S. M. Qaim, Phys. Rev. C **49**, 1525 (1994).
[3] S. Sudár and S. M. Qaim, Phys. Rev. C **53**, 2885 (1996).
[4] B. Strohmaier, M. Fassbender, and S. M. Qaim, Phys. Rev. C **56**, 2654 (1997).
[5] S. M. Qaim, S. Sudár, and A. Fessler, Radiochim. Acta **93**, 503 (2005).
[6] W. Dilg, W. Schantl, and H. Vonach, Nucl. Phys. A **217**, 216 (1973).
[7] K. Hilgers, S. Sudár, and S. M. Qaim, Phys. Rev. C **76**, 064601 (2007).
[8] S. Sudár and S. M. Qaim, Phys. Rev. C **73**, 034613 (2006).
[9] M. Al-Abyad, S. Sudár, M. N. H Comsan, and S. M. Qaim, Phys. Rev. C **73**, 064608 (2006).
[10] V. Avrigeanu, T. Glodariu, A. Plompen, and H. Weigmann, *Proceedings of the International Conference on Nuclear Data for Science and Technology*, Tsukuba, Japan, October 2001; J. Nucl. Sci. Technol., Suppl. 2, 746 (2002).
[11] S. I. Al-Quraishi, S. M. Grimes, T. N. Massey, and D. A. Resler, Phys. Rev. C **67**, 015803 (2003).
[12] *ENDF/B-VII, 2006. National Nuclear Data Center*, Brookhaven National Laboratory, Upton, NY; database version of December 15, 2006.
[13] A. A. Filatenkov and S. V. Chuvaev, Leningrad Report No. 259, *Khlopin Radium Institute*, St. Petersburg, 2003 (unpublished).
[14] F. Tárkányi, K. Gul, A. Hermanne, M. G. Mustafa, F. M. Nortier, S. M. Qaim, B. Scholten, Yu. Shubin, S. Takács, and Y. Zhuang, IAEA-TECDOC-1211, pp. 49–152, 2001; [http://www-nds.iaea.org/medical/monitor_reactions.html].
[15] M.S. Uddin, B. Scholten, A. Hermanne, S. Sudár, H. H. Coenen, and S. M. Qaim, Appl. Radiat. Isot., **68**, 2001 (2010).
[16] S. Y. F. Chu, L. F. Ekstrom, and R. B. Firestone, Lund/LBNL Nuclear Data Service, Version 2.0, 1999; [http://nucleardata.nuclear.lu.se/nucleardata/toi/].
[17] S. Mirzadeh, L. F. Mausner, and M. A. Garland, in *Handbook of Nuclear Chemistry*, edited by A. Vértes, S. Nagy, and Z. Klencsár (Kluwer, Dordrecht, The Netherlands, 2003), vol. 4, p. 1.
[18] A. J. Koning, S. Hilaire, M. C. Duijvestijn, TALYS-*1.0, Proceedings of the International Conference on Nuclear Data for Science and Technology–ND2007*, Nice, France., (EDP Sciences, Les Ulis, France, 2008), p. 211; doi: 10.1051/ndata:07767, @2008 CEA.
[19] J. Raynal, Notes on ECIS94, CEA Saclay Report, No. CEA-N-2772, 1994 (unpublished).
[20] A. J. Koning and J. P. Delaroche, Nucl. Phys. A **713**, 231 (2003).
[21] J. Kopecky and M. Uhl, Phys. Rev. C **41**, 1941 (1990).
[22] D. M. Brink, Nucl. Phys. **4**, 215 (1957).
[23] P. Axel, Phys. Rev. **126**, 671 (1962).
[24] T. Belgya *et al.*, *Handbook for Calculations of Nuclear Reaction Data*, RIPL-2. IAEA-TECDOC-1506 (IAEA, Vienna, 2006). Available online at [http://www-nds.iaea.org/RIPL-2/].
[25] R. F. Coleman, B .E. Hawker, L. P. O'Connor, and J. L. Perkin, Proc. Phys. Soc., London **73**, 215 (1959).
[26] A. K. Hankla, R. W. Fink, and J. H. Hamilton, Nucl. Phys. A **180**, 157 (1972).
[27] N. I. Molla and S. M. Qaim, Nucl. Phys. A **283**, 269 (1977).
[28] L. J. Hua, Z. F. Qun, and K. X. Zhong, Radiochim. Acta **93**, 381 (2005).
[29] *Evaluated Nuclear Structure Data File (ENSDF)*, National Nuclear Data Center, Brookhaven National Laboratory, Upton, NY; [http://www.nndc.bnl.gov/].